J. COMBIN. MATH. COMBIN. COMPUT. 127a (2025) 631–654

Journal of Combinatorial Mathematics and Combinatorial Computing
www.combinatorialpress.com/jcmcc

Combinatorial Press

Analysis of the impact of groundwater seepage on the stability of foundation works in geotechnical engineering

Peng Li[1,✉]

[1] School of Civil and Transportation Engineering of Henan University of Urban Construction Pingdingshan, Henan, 467002, China

ABSTRACT

Groundwater seepage has a greater impact on the stability of foundation engineering, and it is also an important factor that restricts the development of geotechnical engineering projects and the quality of engineering surveys. In this paper, tunnel engineering is selected as the foundation engineering project under study to investigate the specific influence of groundwater seepage in the process of tunnel excavation. The flow-solid coupling model is constructed, and the safety coefficients of the tunnel project in different situations are calculated based on the strength discount method and the ultimate strain method. Numerical analysis software is used to establish the calculation model of the influence of groundwater seepage on the stability of tunnel excavation. The displacement of surrounding rock around the hole is selected as the evaluation index of tunnel stability, and the effect of groundwater seepage on each index is calculated by the analysis software. The study shows that groundwater seepage will make the rock body around the palm face after tunnel excavation change significantly from the pre-excavation bending. The seepage increases the displacement of the surrounding rock, and the coefficient of increase of vertical displacement is larger than the coefficient of increase of horizontal displacement. At the same time, the flow-solid coupling effect of groundwater seepage increases the surrounding rock stress, and the increase coefficients of each key point of the tunnel excavation are between 1.11-1.50, resulting in significant deformation of the bottom of the arch, the top of the arch, and the arch girdle. In addition, the groundwater seepage makes the tunnel safety coefficient decrease from 9.03 to 5.18, which significantly causes the decrease of tunnel stability.

Keywords: groundwater seepage; fluid-solid coupling; strength reduction method; ultimate strain method; foundation engineering stability

1. Introduction

While China's economy continues to develop rapidly, urbanization is being carried out in an orderly manner. With a large number of people pouring into the cities, the problem of alleviating the inconvenient

✉ Corresponding author.
E-mail address: lipeng@huuc.edu.cn (P. Li).
Received 10 July 2024; Revised 11 October 2024; Accepted 29 November 2024; Published Online 15 April 2025.
DOI: 10.61091/jcmcc127a-037

transportation and tight land use has forced a large number of underground projects to be implemented, and many high-rise buildings have risen up [1-2]. These projects in large and medium-sized cities are accompanied by geotechnical engineering, and the depth and difficulty of geotechnical engineering have been increasing. Therefore, foundation engineering stability has become a top priority. Among the various factors affecting the stability of foundation engineering, the destructive effect of groundwater seepage cannot be ignored [3].

The main causes of groundwater seepage problems include the deepening depth of foundation pit excavation and the high and abundant water table in the area [4-5]. When geotechnical engineering is carried out in these areas, groundwater seepage occurs under the action of the huge head difference between inside and outside of the project, resulting in pore water pressure changes in the geotechnical excavation area [6-7]. At the same time in the process of groundwater seepage is often accompanied by seepage erosion problems, mainly manifested as the fine particles in the soil body under the action of infiltration along the pore channels between the coarse particles of the soil body to migrate and lose, the soil skeleton will gradually be hollowed out between the soil skeleton structure, the permeability of the soil body, the density of the soil body and other aspects [8-11]. In addition, groundwater seepage will also cause local settlement of soil and soil stress redistribution [12-13]. The changes of seepage and stress fields not only affect the calculation of lateral pressure of the enclosure structure, but may even cause more serious engineering accidents, thus affecting the stability of the whole foundation project [14-15].

Literature [16] used the stress analysis on the slip surface to study the effect of groundwater seepage on slope stability by constructing a simplified groundwater seepage model, and the results show that the groundwater hydraulic gradient has an effect on slope stability, and the slope with a water table will be damaged to a greater extent. Literature [17] conducted a series of experimental studies on the basic mechanism, numerical simulation and engineering application of the flow in fissured rock, analyzed the microscopic mechanism, characterization method and numerical modeling of fluid flow in fissured rock under a variety of complex conditions, and provided a theoretical basis for seepage and deformation control in geotechnical engineering projects. Literature [18] takes one-dimensional steady state seepage of groundwater as the research condition, establishes a tunnel groundwater seepage drainage model, takes a tunnel project as an example, analyzes the influence of seepage on the effective stress of the ground around the tunnel, and calculates the ground settlement caused by seepage. Literature [19] evaluates the proposed limit support pressure calculation model for the working face of shield tunnels, which is based on the three-dimensional head distribution model and the limit analysis upper limit theorem, and can accurately solve the influence of various factors on the stability of the working face of tunnels. Literature [20] shows that the seepage-damage coupling effect will cause the surrounding geotechnical instability during the excavation of underground cavern, using the elastic-brittle damage model, calculating the radius of the surrounding rock damage area under different conditions with the pore water pressure and the change rule of excavation radius, to provide guidance and reference for similar geotechnical projects. Literature [21] studied the influence of seepage on the working face support pressure and ground collapse mode in shallow buried shield tunneling project, and found that seepage increases the ultimate effective soil pressure at the excavation face, and also increases the ultimate collapse range of the soil body in front of the excavation, and with the increase of relative head difference, the ultimate collapse range of the delineated strata has different degrees of influence.

This paper is based on the strength reduction method utilizing the reduced geotechnical parameters and the retrograde initial geostress equilibrium. The seepage mode is invoked to assign values to parameters such as permeability coefficient of surrounding rock, porosity, fluid modulus, etc. by using FISH language to write programs. After turning on the seepage mode, the fluid-structure coupling model was used to calculate the fluid-structure coupling effect. The safety coefficient of foundation engineering is obtained through the relationship curve between the reduction factor and displacement. In order to present the influence of groundwater seepage on the stability of foundation engineering and the degree, this paper selects the tunnel as the foundation engineering of the study, and uses the numerical analysis software

FLAC3D to carry out numerical simulation, and establishes the model of the influence of groundwater seepage on the stability of the tunnel. The peripheral rock displacement, peripheral rock strength and peripheral rock safety coefficient are used as evaluation indexes to measure the stability of the tunnel, and analyze the specific influence of groundwater seepage on the three indexes of the fluid-solid coupling effect. According to the calculation results, the impact of groundwater infiltration on tunnel stability is visualized, which provides a direction guide for the stability construction of foundation works in geotechnical engineering.

2. Strength discounting method based on coupled fluid-structure modeling

2.1. *Flow-solid coupling model*

"Coupling" refers to the interaction between different fluid flows and the equilibrium conditions of a soil structure, i.e., the solution of the continuity and equilibrium equations [22]. The coupling in this paper is the solution formed by the continuity equation of the seepage field and the equilibrium equation of the stress field and the corresponding boundary and initial conditions.

The equilibrium equation is:

$$\left.\begin{aligned} \frac{\partial \sigma_x}{\partial x}+\frac{\partial \tau_{xy}}{\partial y}+\frac{\partial \tau_{xz}}{\partial z}&=0 \\ \frac{\partial \tau_{xy}}{\partial x}+\frac{\partial \sigma_y}{\partial y}+\frac{\partial \tau_{yz}}{\partial z}&=0 \\ \frac{\partial \tau_{xz}}{\partial x}+\frac{\partial \tau_{yx}}{\partial y}+\frac{\partial \sigma_z}{\partial z}&=-\gamma \end{aligned}\right\} \tag{1}$$

where γ is the bulk weight of the soil and the stress is the total stress. Eq. (1) can also be written as:

$$[\partial]^T+\{\sigma\}=\{f\} \tag{2}$$

where $\{f\}$ is the 3-direction body force.

2.1.1. Effective stress equation. The total stress σ is the sum of the effective stress σ' and the pore pressure u, i.e.:

$$\begin{aligned} \{\sigma\}&=\{\sigma\}+\{M\}u \\ \{M\}&=[111000]^{\mathrm{T}} \end{aligned} \tag{3}$$

Then the equilibrium equation can be written as:

$$[\hat{o}]^T\{\sigma'+[\partial]^T\{M\}u=\{f\} \tag{4}$$

The intrinsic equations are the physical equations:

$$\{\sigma\}=[D]\{\varepsilon\} \tag{5}$$

where D is the stiffness matrix.

2.1.2. Geometric equations. Under the small deformation condition, the geometric equations are:

$$\{\varepsilon\}=-[\partial]^T\{w\} \tag{6}$$

where w is the displacement, i.e., $\{w\}=\begin{bmatrix} w_x \\ w_y \\ w_z \end{bmatrix}$ is the x,y,z-direction displacement component.

2.1.3. Continuity equations. The continuity equation is:

$$\frac{\partial \varepsilon_v}{\partial t} = -\frac{1}{\gamma_w}\left(K_x \frac{\partial^2 u}{\partial x^2} + K_y \frac{\partial^2 u}{\partial y^2} + K_z \frac{\partial^2 u}{\partial z^2}\right) \tag{7}$$

Where, ε_v is the volumetric strain of the soil; γ_w is the bulk weight of the water. K_x, K_y, K_z is the permeability coefficient in x, y, z directions respectively.

$$\varepsilon_e = \{M\}^T \{\varepsilon\} = -\{M\}^T [\partial]\{w\} \tag{8}$$

If $K_x = K_y = K_z = K$, then Eq. (7) can be simplified to:

$$\frac{\partial \varepsilon_v}{\partial t} = -\frac{K}{\gamma_w} \tag{9}$$

where $\nabla = \frac{\partial^2}{\partial x^2} + \frac{\partial^2}{\partial y^2} + \frac{\partial^2}{\partial z^2}$, is called the Laplace operator.

Then the equilibrium differential equation expressed in terms of displacement and pore pressure is:

$$[\dot{o}]^T [D][\partial]\{w\} + [\partial]^T \{M\}u = \{f\} \tag{10}$$

The continuous differential equation expressed in terms of displacement and pore pressure is:

$$-\frac{\partial}{\partial t}\{M\}^{\mathrm{T}} [\partial]\{w\} + \frac{K}{\gamma_w} \hat{\nabla} u = 0 \tag{11}$$

Associative equations (10) and (11) are obtained:

$$\begin{cases} [\partial]^T [D][\partial]\{w\} + [\partial]^T \{M\} u = \{f\} \\ -\dfrac{\partial}{\partial t}\{M\}^T [\partial]\{w\} + \dfrac{K}{\gamma_w} \forall u = 0 \end{cases} \tag{12}$$

Eq. (12) is the coupled equation for the final required solution.

2.1.4. Boundary and initial conditions. Boundaries include stress and displacement boundaries in the stress field and two types of boundaries in the seepage field, i.e., type 1 boundary conditions (given head boundary) and type 2 boundary conditions (given flow boundary). The initial condition of the seepage field is the state of the seepage field at the initial moment (generally taken as $t = 0$), i.e., $h(x, y, z, t)|_{t=0} = h_0(x, y, z, t)$.

2.2. *Strength reduction method and realization process*

2.2.1. Strength reduction method. In the computational analysis of the strength discounting method [23], the strength parameters of the geotechnical body are discounted using equation (13):

$$c' = \frac{c}{F}, \tan\varphi' = \frac{\tan\varphi}{F} \tag{13}$$

The discounted parameters are substituted into the numerical model for calculation, and the limit state on the verge of destruction is obtained by gradually increasing the discount coefficient, and the discount coefficient corresponding to this state is the safety coefficient.

2.2.2. Realization process. Most of the foundation engineering damage belongs to shear damage, tensile strength reduction or not on the foundation engineering safety coefficient has a small impact, this paper only on the foundation engineering shear strength parameters c and φ reduction, the calculated safety coefficient for the shear safety coefficient. The specific realization process is as follows, before the fluid-structure coupling analysis using the discounted geotechnical parameters for the initial ground stress balance, and the calculated nodal displacements, velocities and plastic zones are initialized. Subsequently, the seepage model is invoked, and the surrounding rock is set as an isotropic seepage model, and the permeability coefficient, porosity, fluid modulus, fluid tensile strength, fluid density, and pore water pressure of the surrounding rock are assigned using the program written in FISH language. The construction of foundation engineering was simulated by passivating the foundation engineering unit, and the pore water pressure at the perimeter boundary of the foundation engineering was set to 0. Subsequently, the seepage mode was turned on to carry out the fluid-solid coupling calculation. By gradually increasing the reduction factor, the displacement of the characteristic points of the foundation engineering is obtained with the change curve of the reduction factor. The displacement of the characteristic points of the foundation project is obtained by gradually increasing the reduction factor, and the reduction factor corresponding to the position where the displacement-reduction factor curve changes abruptly is the safety factor of the foundation project.

2.2.3. Modeling the effect of groundwater infiltration on the stability of foundation works. The hydrogeological conditions faced by tunnels in the construction process are complex and variable, and a large number of engineering practices in various countries have shown that tunnels are often prone to engineering disasters such as water gushing, mudsurge and even landslides when they pass through water-rich areas, so it is necessary and practical to carry out the study on the impact of groundwater infiltration on the stability of water-rich tunnels under the effect of fluid-solid coupling. Therefore, this paper selects the tunnel as the basic engineering research object, evaluates its stability using indicators, and simulates the effect of groundwater infiltration on the stability evaluation indicators of the tunnel using numerical computation methods.

2.3. *Overview of the Tunnel Project*

2.3.1. Brief description of the project. The construction of the first phase of a city's rail transit line 1 began in 2015, and it is planned to be completed for trial operation by the end of 2017. The line starts from station A in the east and goes to station B in the west, with a total length of 23.76 kilometers, all of which are laid underground, with a total of 15 stations, with an average station spacing of 1.58 kilometers and a maximum spacing of 2.49 kilometers.

Station C ~ Station D interval is a section of the city's urban rail transit line one project. The design mileage of the right line of the interval is: YCK13+138.752~YCK15+049.374, with a line length of about 1.83 kilometers. The design mileage of the left line is: ZCK13+138.752~ZCK15+049.374, the line length is about 1.83 kilometers. A part of the line in the zone has to go through the Yellow River, which flows through the city in the direction from west to east. The tunnel through the Yellow River is constructed by a continuous mud-water pressurized balanced shield machine, and the shield boring schematic is shown in Figure 1. The mileage of the right line of the underwater tunnel is YCK13+81.64~YCK14+221.38, and the mileage of the left line of the underwater tunnel is ZDK13+713.57~ZDK14+309.42, and the length of the tunnel is about 387 m. The tunnel is tunneling in the direction of station C to station D, and the tunnel adopts a double-hole arrangement.

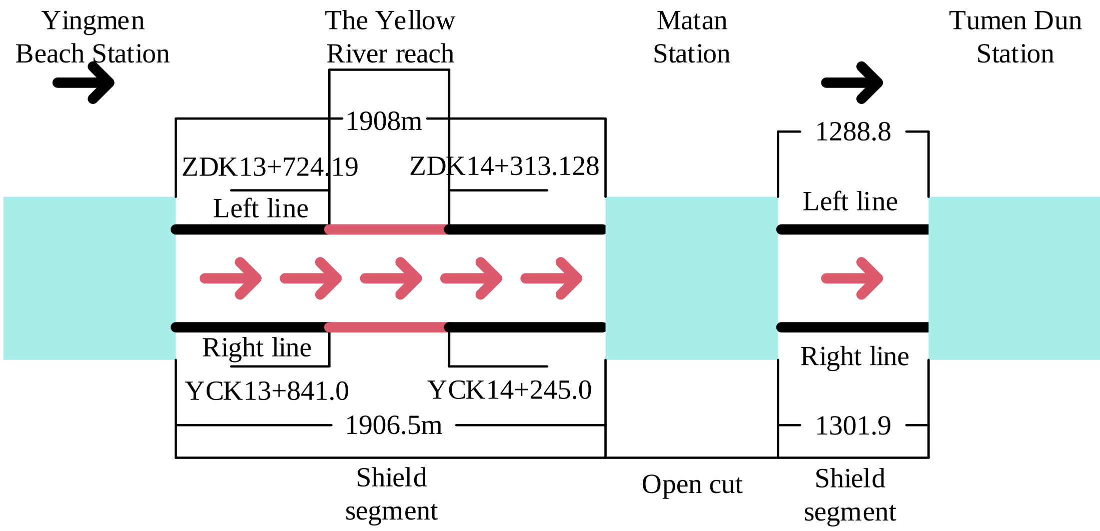

Fig. 1. Schematic diagram of tunneling in shield zone

The maximum excavation diameter of the shield machine is 5.84m, and the pipe sheet is a universal pipe sheet: 3 (standard block) + 2 (neighboring block) + 1 (K block), assembled with staggered seams (through-seam assembly at the contact channel), and connected with M30 curved bolts. The outer diameter of pipe sheet is 5.71m, inner diameter is 5.58m, the ring width of pipe sheet is 1.5m, thickness is 0.27m, the length of shield machine is about 8.3m, and the length of the whole shield machine is about 91.82m. 280 rings of pipe sheet are needed by 2 sets of mud-water shield machine in the section of passing through the yellow zone between station C and station D on average per month, and the maximum demand for pipe sheet per month during the excavation period can be calculated according to the speed of excavation and the site storage condition, which is calculated according to the maximum demand for 480 rings of pipe sheet per month. The maximum monthly demand of pipe sheets can be calculated according to 480 rings. The total number of pipe sheets for tunneling through the yellow tunnel in this section is 652 rings.

2.3.2. Hydrogeology:

1) Geological situation. The tunnel under the Yellow River section mainly passes through the area of loose pebble layer. According to the preliminary geological survey report, the cross section of the project river section is extremely irregular. Due to sand mining and sand extraction for construction of wetland park on the left bank beach, there is a deep pool of stagnant water on the beach by the main stream, and there is an artificially excavated pool of about 200m long and 150m wide in the beach. The project crosses the location of the beach with a width of nearly 180m, and there exists a deep channel of stagnant water with a depth of 4m, a width of about 60m, and a length of 800m, and the beach is overgrown with reeds, bushes, and weeds. This interval tunnel goes down through the Yellow River from 35m to 40m upstream of Yintan Bridge, and the length of the bed of the Yellow River is 392.43m, in which the width of the Yellow River is about 193m. The top plate of the tunnel is 17.34m~23.58m away from the bottom plate of the riverbed.

The strata of the interval from Station C to Station D are: artificial fill distributed on the surface, alluvial medium sand and pebbles of the Holocene of the Quaternary System and pebbles of the Lower Pleistocene of the Quaternary System, respectively. The stratum of the site is divided into 4 layers from top to bottom, and the thickness of each layer is 0.5m~8.2m, 1.5m~1.8m, 2.5m~13.7m and 2.5m~13.7m respectively.

According to the geological exploration drawings and design drawings of the first phase project of the city's rail transit line 1, the shield machine is basically in the pebble layer within the scope of the section of the Yellow River, the geology of this stratum is relatively complex, and the groundwater content of this stratum is extremely rich and the dive through the pore space of the pebble layer is intercommunicated with the groundwater, and the probability of the risk of gushing water, gushing sand, the ground surface of the bottom of the river settling or bulging, and the risk of loss of pressure of excavation bins is extremely high in the shield tunneling process.

2) Hydrological conditions:

(1) Elevation of groundwater level. During the survey period of the proposed site, the water level of the Yellow River was 1478.9m, and the elevation of the groundwater level ranged from 1473.6m to 1482.8m, and the groundwater level has a tendency of decreasing slowly from north-west to south-east.

(2) Distribution of aquifers. Groundwater is mainly stored in the pebble layer, which is a river valley porous diving, and the thickness of the aquifer is 150m~320m according to the investigation data in the feasibility study stage.

(3) Recharge, runoff and discharge of groundwater. The direction of groundwater runoff in this zone is from north-east to south-west. North of the Yellow River, groundwater is mainly recharged by atmospheric precipitation and surface water infiltration, and is discharged in the Yellow River; south of the Yellow River, groundwater is mainly recharged by atmospheric precipitation, surface water infiltration, and the Yellow River, and is discharged by artificial mining and underground overflow.

According to the comprehensive study report of urban environmental geology, the city of the Yellow River Ⅱ terrace zone, groundwater dynamics is mainly affected by seasonal changes, the water level change range is generally 0.8m ~ 1...2m, the high water level period of about 3 months (June ~ August), seasonal changes are obvious.

(4) Value of permeability coefficient. According to the site hydrogeological conditions and aquifer material composition, combined with regional engineering experience, the value of permeability coefficient of each soil layer is 4m/d~6m/d for miscellaneous fill, 30m/d~50m/d for pebbles.

(5) Prediction of pit water influx. The depth of the tunnel main structure base plate is 12.9m~31.8m, the diameter of the single hole is 5.7m, the groundwater level is higher than the elevation of the tunnel roof, the tunnel body mainly passes through the pebble layer through the yellow tunnel, and there is the problem of tunnel water influx during the construction of the tunnel using the shield method. Calculation formula of tunnel water influx in the single line of the interval is based on the non-complete calculation formula of groundwater to estimate the tunnel water influx in the interval from station C to station D. According to the hydrogeological conditions and the shield construction method, and taking into account the annual change of groundwater level of the site of 1.8m, the groundwater level used in the calculation is the average water level of the current survey plus 1.3m, and the results of the calculations are shown in Table 1.

Table 1. Estimate of tunnel inflow (Single wire tunnel)

Tunnel length(m)	H(m)	K(m/d)	I	A(m2)	Q(m3/d)
292.82	13.66	79.00	0.13	15.29	6.28
206.65	21.70	58.26	0.63	20.2	4.85
200.91	22.31	60.79	0.75	20.65	6.78
396.25	26.86	100.01	0.32	24.93	0.65
180.89	27.53	58.26	0.49	27.34	9.25
232.96	24.17	58.74	0.24	25.20	9.54
199.89	14.95	58.33	0.43	18.19	5.96
195.69	10.85	58.96	0.48	10.73	1.85

2.3.3. Construction program:

1) Shield tunneling operation. When shield tunneling, the management benchmark is set first, and then tunnel excavation is carried out, and synchronized grouting is carried out at the same time of excavation. The soil generated by excavation is transported to the designated location by transportation vehicles, and if the excavation depth does not reach the position of the circular footage, the excavation will continue, and when the excavation footage reaches a certain cyclic footage, the pipe pieces will be assembled, and then the next cyclic footage of excavation will be carried out, and then the pipe pieces will be assembled, until the excavation is completed by assembling the last ring of pipe pieces, and at this time, the shield tunnelling work is completed.

2) Synchronized grouting. This tunnel construction uses synchronized gradual mixing equipment, slurry ratio is cement: 180~220kg, fly ash: 180~280kg, bentonite: 150~180kg, sand: 590kg, water: 330~390kg, additives are added according to actual experimental requirements.

As the outer diameter of shield is larger than the diameter of pipe sheet, in the construction process, the soil on the excavation surface and the pipe sheet will produce a certain volume of void between them, which affects the supporting role of the pipe sheet and construction safety. The construction process is carried out by synchronized grouting, so that the gap between the pipe sheet and the soil can be filled by slurry to ensure construction safety. During construction, the way of advancing and grouting linkage is adopted, and the schematic diagram of the grouting system is shown in Figure 2.

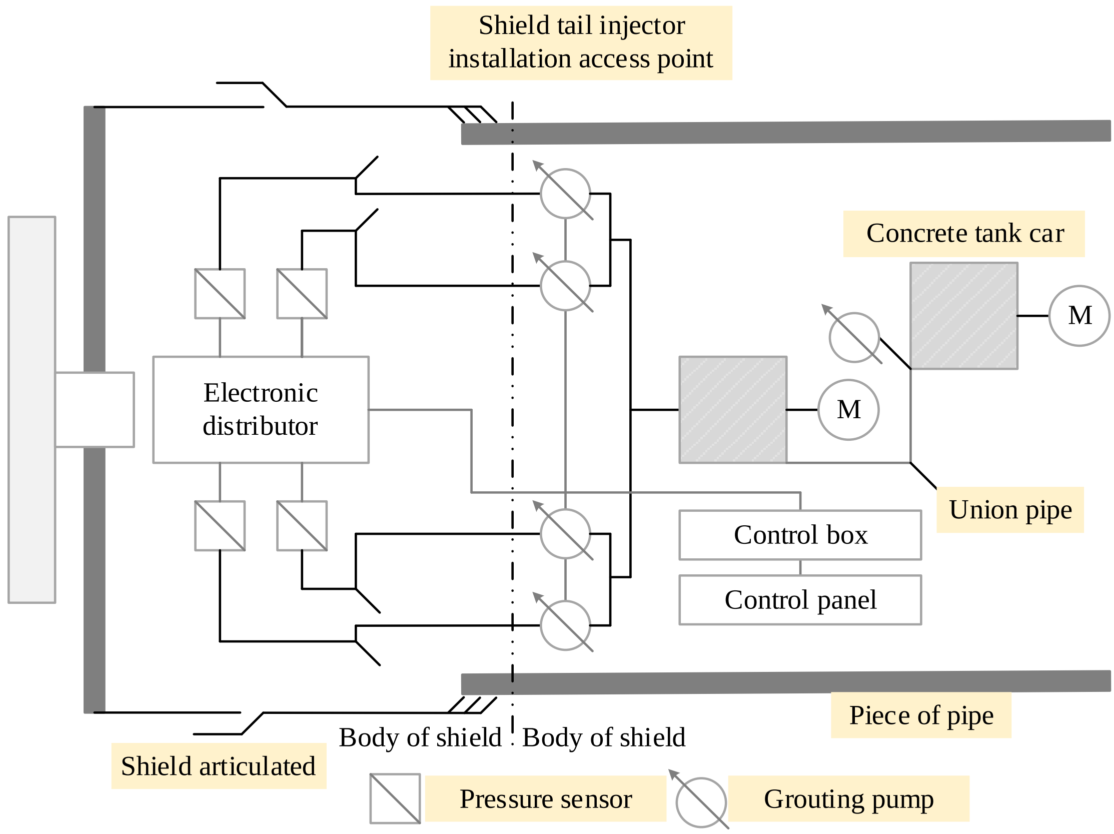

Fig. 2. Schematic diagram of grouting system

In order to ensure that the slurry can fill the gap between the pipe sheet and the soil body to the maximum extent, i.e., to let the grouting effect reach the best, the grouting pressure in this grouting takes the value of 0.3-0.8MPa, and the grouting volume of each assembled ring of pipe sheet (width of 1.4m) is Q=4.2-5.7m^3. When the grouting volume reaches more than 80% of the design value, it can be considered that the quality requirements have been met. If the geological gap changes in different mileage sections, the parameters of grouting gap should be adjusted in time and increased to 1.5 times if necessary. Grouting effect check mainly adopts analytical method and non-destructive detection method for effect check and comprehensive analysis and judgment.

2.4. Numerical simulation program

2.4.1. Computational modeling. The calculation model was established by numerical simulation software FLAC3D. In the model, the level is 80m from the tunnel center line to each side, the arch is 48m from the top of the model and 32m from the bottom of the model, the model is 100m along the tunnel excavation direction, divided into 50 2m excavation scales, and the model range is 120m × 120m × 90m. The thickness of the tunnel initial support is 0.37m, and the thickness of the second lining is 0.83m. The front, back and left boundaries of the model are set up with normal displacement constraints, and the top of the model is a free boundary. The top is free and the bottom is fixed. The seepage model adopts isotropic seepage model, and the bottom, front, back, left and right boundaries of the model are impermeable boundaries. In order to simulate the phenomenon of groundwater discharge during tunnel construction, the contact surface of the primary support and the second lining of the tunnel is set as a permeable boundary with a pore water pressure of 0MPa. Before tunnel construction, the surrounding rock is assumed to be water-saturated.

The boundary of the model without considering fluid-solid coupling is the same as that of the fluid-solid coupling model, with normal constraints set at the front and rear boundaries, and the bottom is set as a fixed boundary. Since the seepage of groundwater is not considered, the model does not carry out seepage calculations, and the seepage boundary is not set. In order to more comprehensively study the influence of the fluid-solid coupling effect on the surrounding rock and the supporting structure, the simulation adopts the CRD method to verify the conclusions [24].

2.4.2. Model calculation parameters. The surrounding rock is modeled using the M-C ontological model, and the grouted reinforcement ring is simulated by changing the soil parameters without considering the separate action of the grouted anchors, which are equivalent to the strength of the grouted rock. The initial support is modeled by the ideal elasticity principal model, and the 120 steel frame is discounted to the initial support according to the equivalence principle. The temporary support is thin relative to the model and is simulated using shell units.The I20a steel frame is converted according to the principle of equivalence of flexural strength, which is given in Eq:

$$E = E_c + \frac{E_g S_g}{S_c} \tag{14}$$

Where: E - is the modulus of elasticity of the initial support after equivalence. E_c - is the concrete modulus of elasticity. E_g - is the modulus of elasticity of steel frame. S_g - is the cross-sectional area of steel frame. S_c - is the concrete cross-sectional area.

The parameters of the surrounding rock as well as the supporting structure are jointly determined according to the "Design Code for Highway Tunnels" (JTG33701-2018) as well as the detailed geotechnical investigation report of the tunnel project (tunnel section), and the specific settings are shown in Table 2.

Table 2. Model calculation parameter

Type	Surrounding rock	Grouting ring	Initial branch	Temporary support
Elastic modulus E/GPa	1.70	4.60	25.48	26.82
Poisson ratio μ	0.37	0.24	0.18	0.23
Bulk weight γ/(KN/m3)	21.48	22.52	24.98	25.04
Cohesive force c/MPa	0.27	0.53	/	/
Interior friction Angle ψ/(°)	33	39	/	/
Porosity	0.3	0.3	0.2	/
Permeability coefficient K/(m/s)	1.48×10-6	3.43×10-7	0.96×10-8	/

2.4.3. Tunnel Monitoring Points. In order to minimize the error brought by the boundary effect on the calculation results, the monitoring section was set at Y=50m in the middle of the model. The specific coordinates of each deformation monitoring point in the xOz plane are GD01 (0,0), SL01 (-6.7,-4.8), SL03 (6.7,-4.8), and GD02 (0,-10.4), and the specific coordinates of the perimeter rock stress monitoring points are the top of the arch (0,0), the left arch waist (-5.9,-2.3), left arch foot (-7.4,-8.6), arch bottom (0,-10.4), and the initial support stress monitoring points are inside the corresponding points.

2.4.4. Flow-solid coupling calculation model. In FLAC3D, the flow-solid coupling calculation modes are mainly categorized into complete flow-solid coupling calculation and incomplete flow-solid coupling calculation, and three factors are mainly considered when making mode selection:

1) Ratio of mechanical perturbation time t_s to coupled diffusion characteristic time t_c. The time required for the mechanical analysis of tunnel excavation perturbation in FLAC3D is very short compared

to the coupled diffusion characteristic time, i.e., $t_c >> t_s$. Therefore, the influence of seepage on the calculation results can be basically ignored at the moment of excavation, and the stress release process of tunnel excavation can be regarded as a short-term behavior (without draining), and only the mechanical calculation is opened.

2) Characterization of perturbations to the coupling process. In the fluid-solid coupled system, different perturbations have different effects on the boundary conditions. In this paper, the tunnel excavation belongs to mechanical perturbation, which will lead to the change of the mechanical boundary of the model, while the perturbation generated by grouting belongs to fluid perturbation, which changes the seepage boundary. However, since the overrun grouting does not change the size of the pore pressure, the actual impact is almost negligible, so the fluid-solid coupling system in this paper can be regarded as only enforced mechanical perturbation, in which case the selection of computational model needs to depend on the fluid-solid stiffness ratio.

3) Stiffness ratio R_k. The stiffness ratio R_k is important for the selection of the flow-solid coupling calculation mode. When $R_k << 1$ that the rock medium is a rigid skeleton, the diffusion process of pore pressure can be uncoupled, and the calculation of the seepage field can be carried out separately, using the calculation mode of incomplete fluid-solid coupling. When $R_k >> 1$, i.e., the rock medium is a flexible skeleton, the calculation mode of complete fluid-solid coupling should be adopted. The specific calculation formula for the fluid-solid stiffness ratio R_k is as follows:

$$R_k = \frac{\alpha^2 M}{K + 4G/3} \tag{15}$$

Where $M = K_f / n$, porosity n for 0.2, fluid bulk modulus at room temperature K_f for 2.0GPa, so the fluid modulus M = 10Gpa. α for the Bio-modulus, this paper assumes that the fluid is incompressible, so the $\alpha = 1$. K, G for the volume modulus and shear modulus of the geotechnical body, respectively, substituting into the parameters of the perimeter rock is calculated as K for 2.14GPa, G for 0.66GPa, according to the above formula to calculate the final flow-solid stiffness ratio of $R_k = 3.31 >> 1$, and therefore the need to Therefore, it is necessary to use the complete fluid-solid coupling calculation model.

In this paper, it is assumed that the tunnel is grouted 50m ahead of the tunnel at one time, and the whole length of the model is grouted twice, once before excavation, and then once after the palm face is advanced 32m. In the numerical simulation, the palm face advances 2m each time, the construction rate is taken as 4m/d, and it is assumed that the rate remains constant throughout the construction process. When the fluid-solid coupling is not considered, no seepage boundary is imposed and no seepage calculation is carried out on this basis.

2.5. *Tunnel Stability Evaluation Indicators*

2.5.1. Indicators for evaluating perimeter displacements of perimeter caves. As a measurable indicator, perimeter rock displacement is the most direct basis for judging the stability of the tunnel after excavation. In this paper, the simulation section of the tunnel depth is less than 80m, in the water-rich area of class IV surrounding rock, according to the "Highway Tunnel Design Code" (JTGD70-2004), the permissible relative horizontal convergence value of the hole perimeter is 0.12% to 0.45%, and the permissible value of the settlement of the arch top is adopted as 0.8-1.2 times of the value of 0.12% to 0.45%. Since the simulated section of surrounding rock is endowed with water-rich environment, it is easy to happen disasters such as mud-surge and water-surge, in order to ensure the safety of tunnel construction, the permissible relative horizontal convergence value around the hole and the permissible value of vault settlement are taken as a small value, i.e., the limit value of horizontal convergence is 23.56mm, and the limit value of vault settlement is 11.48mm.

2.5.2. Enclosed rock strength indicators. In this paper, relying on the IV level peripheral rock in the water-rich area, according to the indoor physical and mechanical test data of the rock in the investigation report, the compressive strength of the peripheral rock after discounting is 9.84MPa, and the tensile strength is 0.31MPa, and the peripheral rock is considered to be destabilized and damaged if the stress of the peripheral rock exceeds this value after tunnel excavation.

2.5.3. Evaluation index of enclosure safety factor. In this paper, on the basis of the strength discount method, the ultimate strain method is adopted to take the penetration of the ultimate shear strain zone of the peripheral rock around the tunnel as the criterion of overall instability [25], because the peripheral rock under the influence of groundwater seepage will produce infiltration and deformation, and at the same time, the decrease of the effective stress in the peripheral rock caused by the pore water pressure will also change the stress-strain relationship, therefore, the safety coefficient of the peripheral rock calculated by the ultimate strain is more representative compared to the other methods. Therefore, the factor of safety of surrounding rock calculated by ultimate strain as evaluation index is more representative than other methods.

3. Analysis of the impact of groundwater seepage on the stability of foundation works

3.1. Pore water pressure field analysis of surrounding rock

Figure 3 shows the initial pore water pressure of the tunnel and the distribution of pore water pressure after tunnel excavation, (a) is the distribution of pore water pressure before excavation and (b) is the distribution of pore water pressure after excavation. From the figure, it can be seen that the surrounding rock is considered to be in a water-saturated state before tunnel excavation, and the pore water pressure distribution layer demarcation line is more obvious, which is a stable seepage field. The pore water pressure near the tunnel excavation palm face decreases, generating a pressure head difference, groundwater infiltration around the tunnel, and the equivalent water pressure line is concave downward around the tunnel. The maximum pore water pressure in the rock body is 0.384MPa. The pore water pressure difference causes the seepage field to change, and the rock body around the palm face after excavation forms obvious changes with the pre-excavation, showing a curve distribution until the groundwater is stabilized again, and then finally forms a funnel-shaped settlement area, and the left and right water pressures are symmetrically distributed.

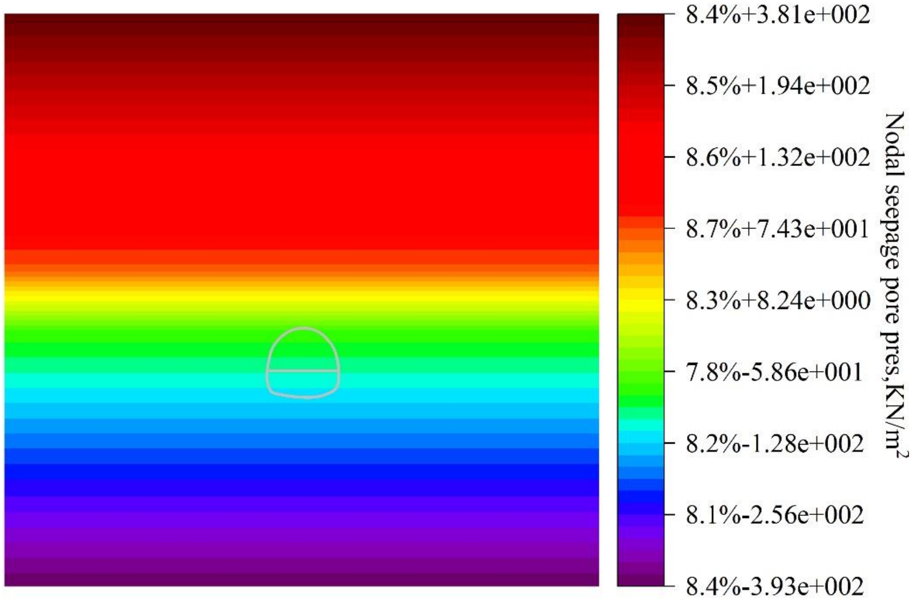

(a) Pre-excavation pore water pressure distribution

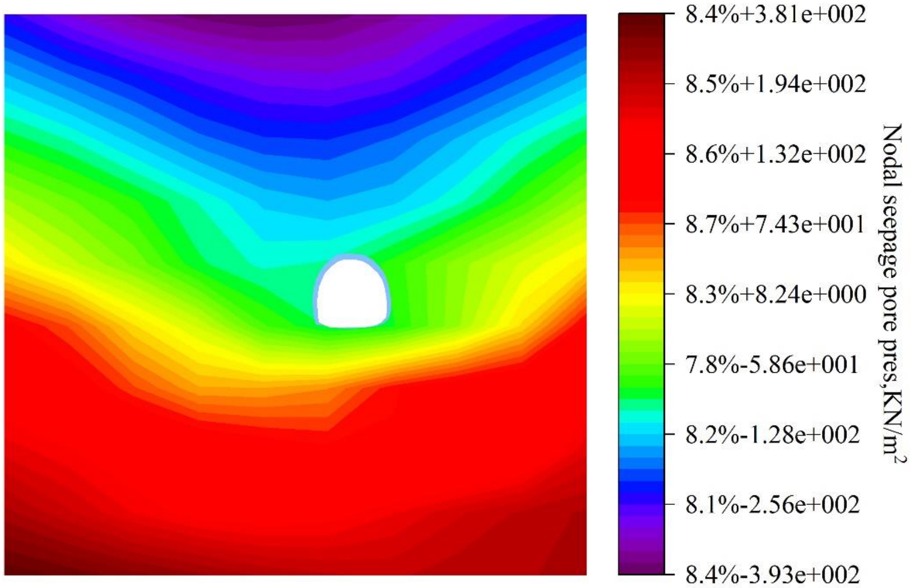

(b) Post-excavation pore water pressure distribution

Fig. 3. Pore water pressure distribution

3.2. Enclosed rock displacement field analysis

The numerical simulation of tunnel excavation is carried out by CRD method, and the surrounding rock is in a relatively stable state under the initial condition, after the initial stress field analysis, the displacement is cleared by checking the displacement in the numerical software, and the vertical displacement and deformation diagrams are shown in Fig. 4 and Fig. 5, of which Fig. 4 is the vertical displacement of the surrounding rock by considering the effect of fluid-solid coupling, and Fig. 5 is the vertical displacement of the surrounding rock by disregarding the effect of fluid-solid coupling. Figures (a) and (b) both indicate the cases of 10m and 20m from the initial excavation face respectively. When the surrounding rock displacement field analysis is carried out, it is considered that the rock body below the water level line is in a saturated state, and after the tunnel is excavated, the stable state of the surrounding rock is broken, the stress is redistributed, and with the change of the seepage field, the vertical displacement and the horizontal displacement gradually increase. From Figures 4 and 5, it can be seen that CRD method tunnel excavation, the maximum vertical displacement occurs in the top and bottom of the arch, and the top of the arch is negative, which represents settlement, and the bottom of the arch is positive, which represents augmentation, and in the range of numerical simulation, the settlement of the top of the arch is increasing with the increase of the tunneling footage.

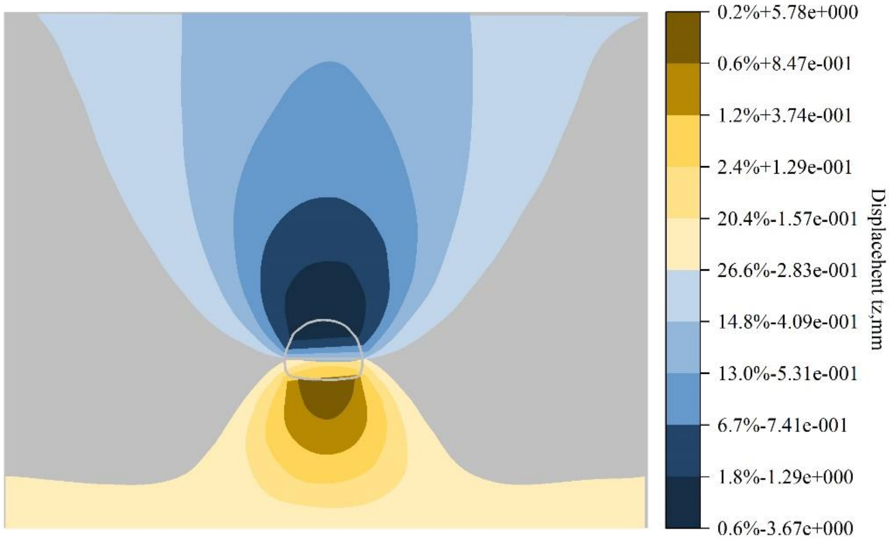

(a) 10 m away from the initial excavation face

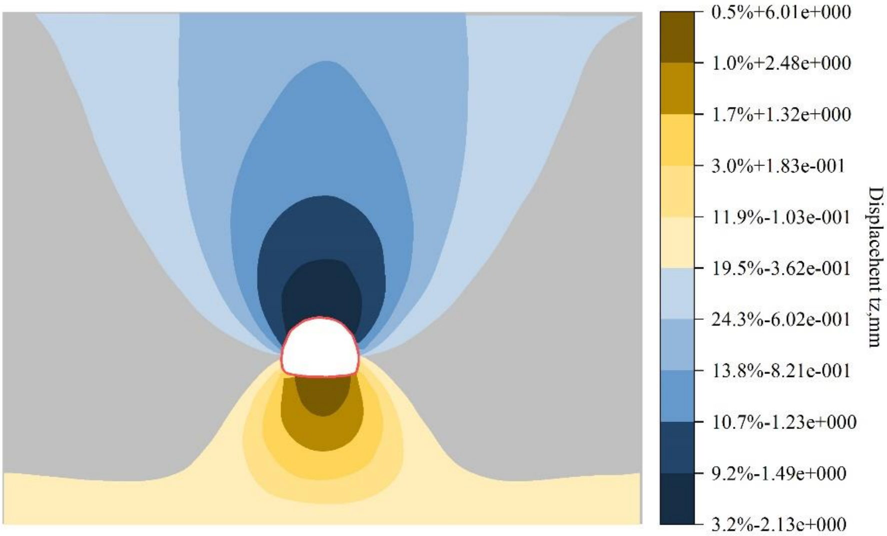

(b) 20 m away from the initial excavation face

Fig. 4. Vertical displacement of surrounding rock with fluid structure coupling

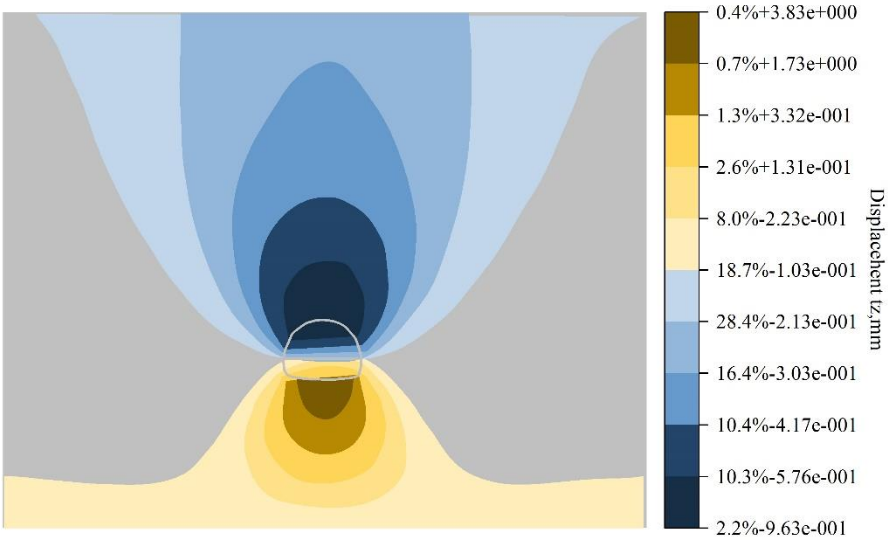

(a) 10 m away from the initial excavation face

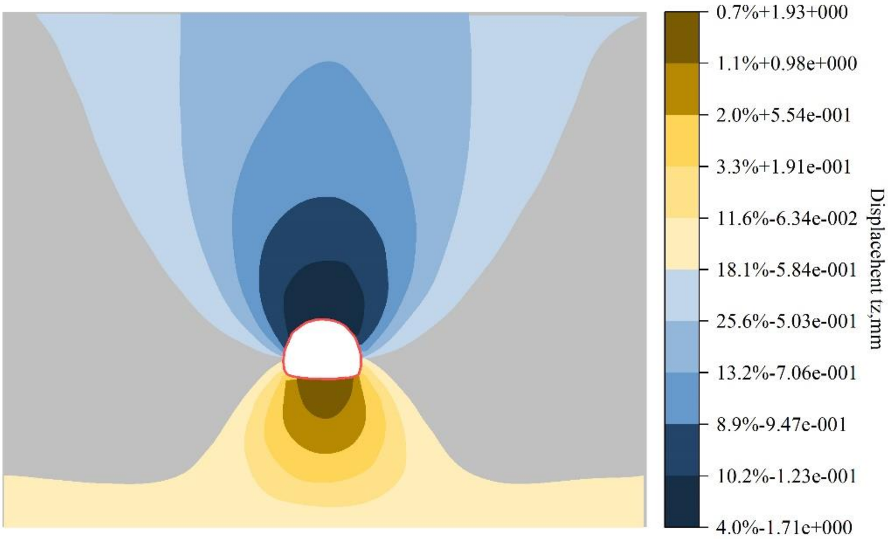

(b) 20 m away from the initial excavation face

Fig. 5. Vertical displacement of surrounding rock without fluid structure coupling

Table 3 shows the results of vertical displacement of surrounding rock in different excavation steps. The maximum settlement of the arch is 3.53 mm and the maximum bulge is 4.12 mm without considering fluid-solid coupling, and the maximum settlement of the arch is 4.68 mm and the maximum bulge is 6.27 mm with considering fluid-solid coupling, compared with the case without considering fluid-solid coupling, considering fluid-solid coupling increases the value of the arch settlement by 1.33 times, and the value of the arch bottom bulge increases by 1.52 times. Whether in the fluid-solid coupling or non-fluid-solid coupling condition, with the increase of excavation footage the settlement of the arch top increases, and the bottom of the arch rises as well. When the excavation reaches 15m, the displacement of the surrounding rock in both conditions is within the permissible range, and the surrounding rock in the fluid-solid coupling condition increases the displacement of the surrounding rock, and the coefficients of increase of the settlement of the arch top range from 1.19 to 1.37, and that of the bottom of the arch rise from 1.14 to 1.52. Before excavation, the slope of change of 12m displacement of arch settlement and arch bottom augmentation is large, and the slope of change of 12m-20m excavation is small, and the curve area is gentle.

Table 3. Vertical displacement of surrounding rock

Distance from the initial excavation face(m)	With fluid coupling		Without fluid coupling		Increase factor	
	Vault settlement	Arch bottom uplift	Vault settlement	Arch bottom uplift	Vault settlement	Arch bottom uplift
2	-1.48	2.08	-1.24	1.82	1.19	1.14
4	-2.52	3.83	-1.96	2.83	1.29	1.35
6	-3.17	5.04	-2.34	3.59	1.35	1.40
8	-3.58	5.63	-2.68	3.72	1.34	1.51
10	-3.86	5.74	-2.82	3.93	1.37	1.46
12	-4.12	5.79	-3.06	4.01	1.35	1.44
14	-4.28	5.98	-3.15	4.03	1.36	1.48
16	-4.37	6.03	-3.29	4.06	1.33	1.49
18	-4.51	6.14	-3.48	4.09	1.30	1.50
20	-4.68	6.27	-3.53	4.12	1.33	1.52

Figures 6 and 7 show the results of horizontal displacement of the surrounding rock considering and not considering fluid-solid coupling, respectively. Table 4 shows the horizontal displacement at the key point after tunnel excavation. After the seepage module is turned on, the horizontal displacement of the left wall at the key point location increases from 0.51 to 0.58, which is 1.14 times larger, the horizontal displacement of the right wall increases from 0.46 to 0.61, which is 1.33 times larger, the horizontal displacement of the left arch foot increases from 0.32 to 0.37, which is 1.16 times larger, and the horizontal displacement of the right arch foot increases from 0.37 to 0.42, which is 1.14 times larger. From the analysis, it can be seen that after the seepage module is turned on, the coefficient of increase of vertical displacement of tunnel excavation is greater than the coefficient of increase of horizontal displacement, so the effect of groundwater seepage has a greater impact on the vertical displacement of the surrounding rock, and the impact on the horizontal displacement is relatively small.

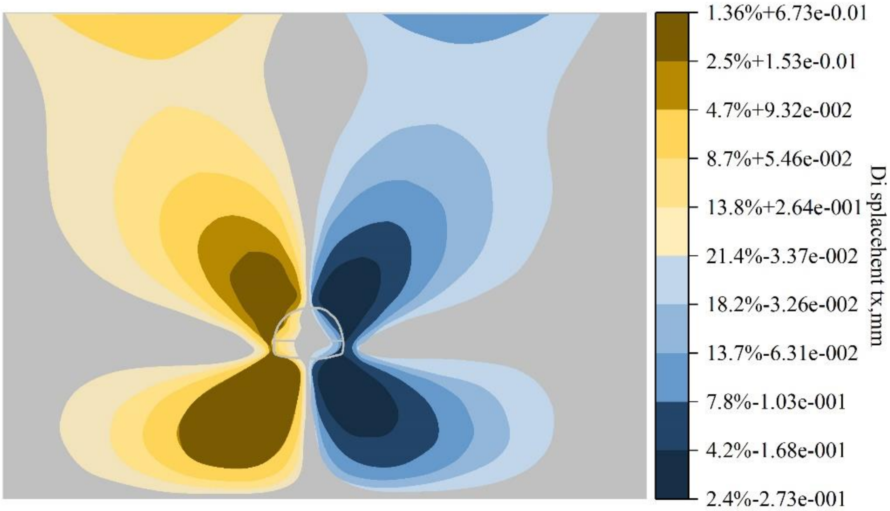

(a) 10 m away from the initial excavation face

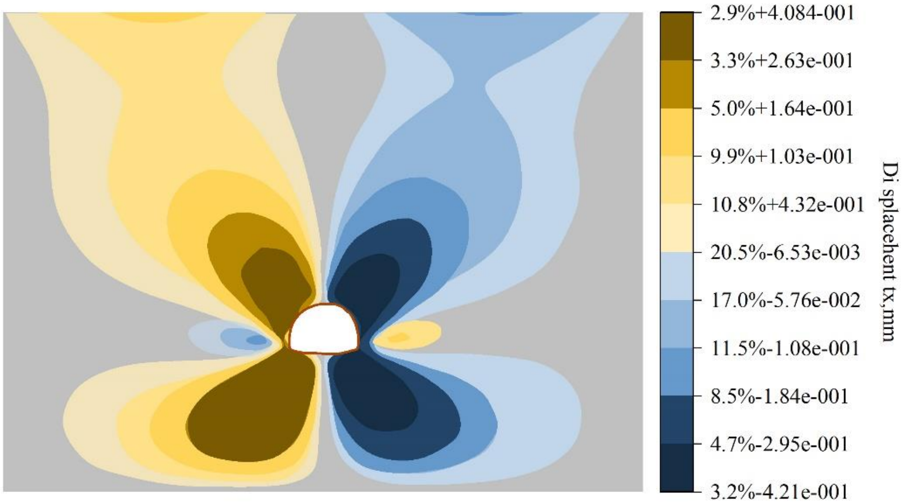

(b) 20 m away from the initial excavation face

Fig. 6. Horizontal displacement of surrounding rock with fluid structure coupling

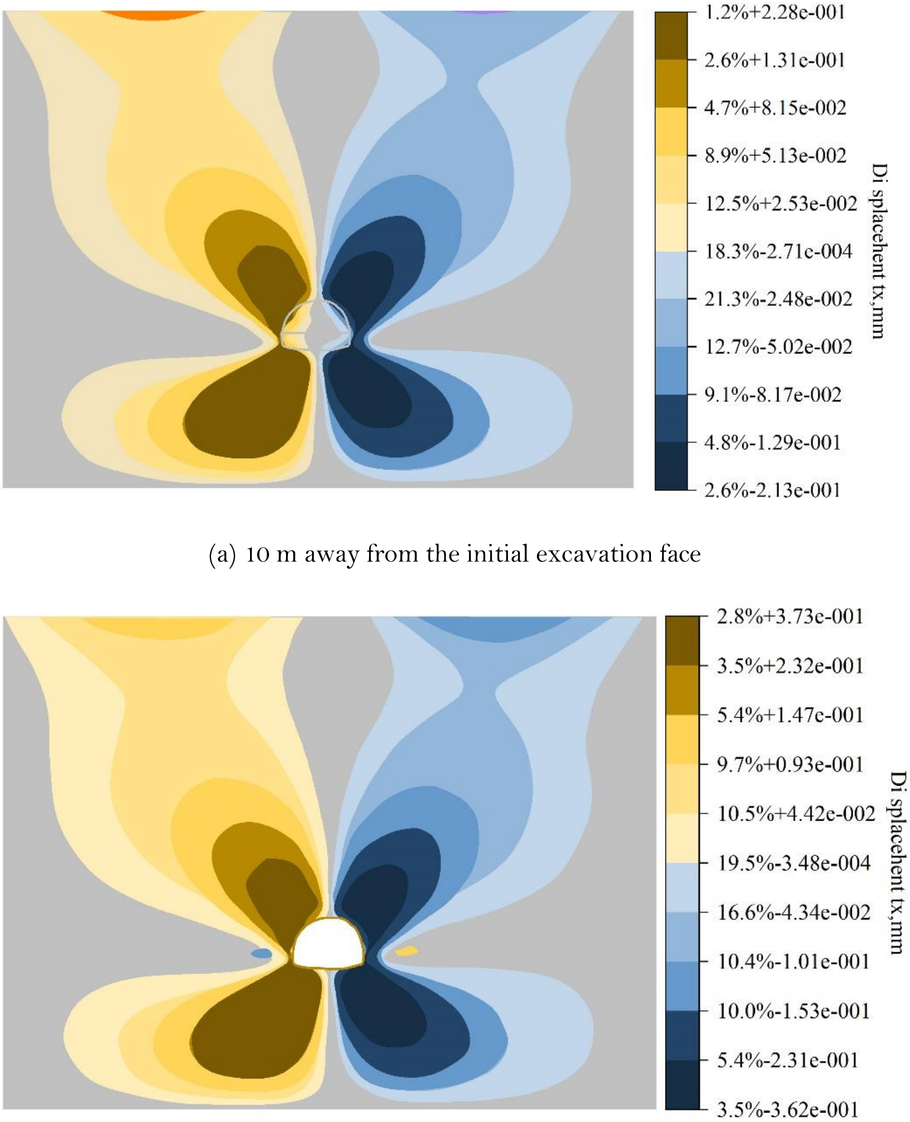

(a) 10 m away from the initial excavation face

(b) 20 m away from the initial excavation face

Fig. 7. Horizontal displacement of surrounding rock without fluid structure coupling

Table 4. Horizontal displacement of key points after tunnel excavation(mm)

Operating condition	With fluid coupling	Without fluid coupling	Increase factor
Left wall	0.58	0.51	1.14
Right wall	-0.61	-0.46	1.33
Left arch	0.37	0.32	1.16
Right arch	-0.42	-0.37	1.14

3.3. *Perimeter rock stress field analysis*

Figures 8 and 9 show the results of the first and third principal stresses after tunnel excavation under two working conditions, respectively, and (a) and (b) both show the surrounding rock stresses under non-fluid-solid coupling and fluid-solid coupling. Simulated by numerical modeling calculation. The first principal stress and the third principal stress of tunnel excavation are obtained, and the performance of the surrounding rock stress considering fluid-solid coupling and not considering fluid-solid coupling morphology is basically similar, but numerically changed, which is due to the fact that after the tunnel excavation, the state of the surrounding rock stress is changed and the state of the ground stress is redistributed. Tunnel excavation wall, only the effect of self-gravity so that the ground stress is horizontally distributed, the stress size and the depth of the surrounding rock has a relationship with the depth of the surrounding rock, roughly equal to the depth and the product of the weight of the surrounding rock. Tunnel excavation in the vertical range of influence is greater than the horizontal range of influence.

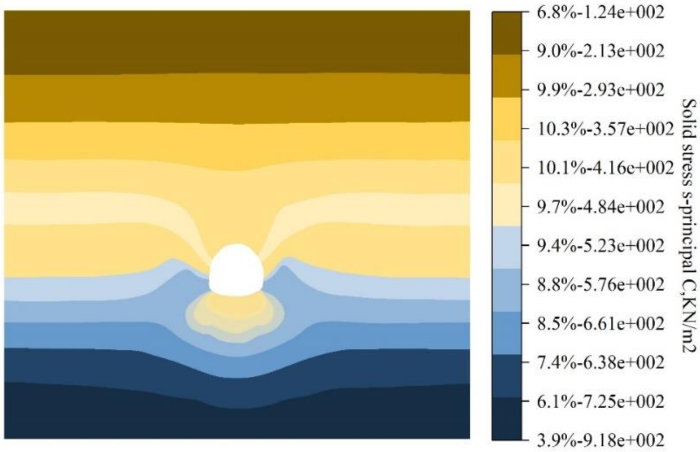

(a) First principal stress of non-fluid solid coupling surrounding rock

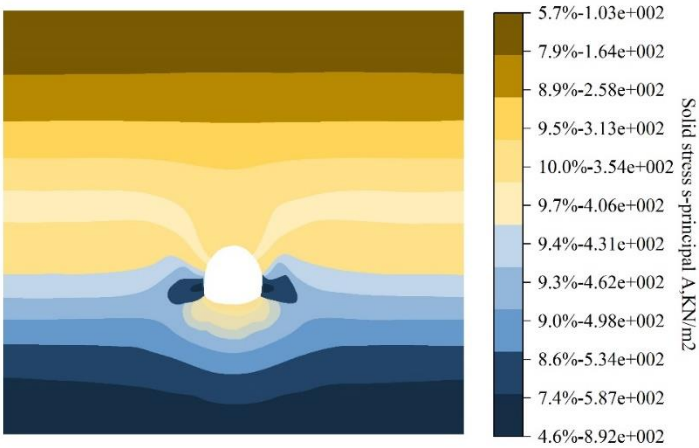

(b) First principal stress of fluid solid coupling surrounding rock

Fig. 8. First principal stress during tunnel excavation

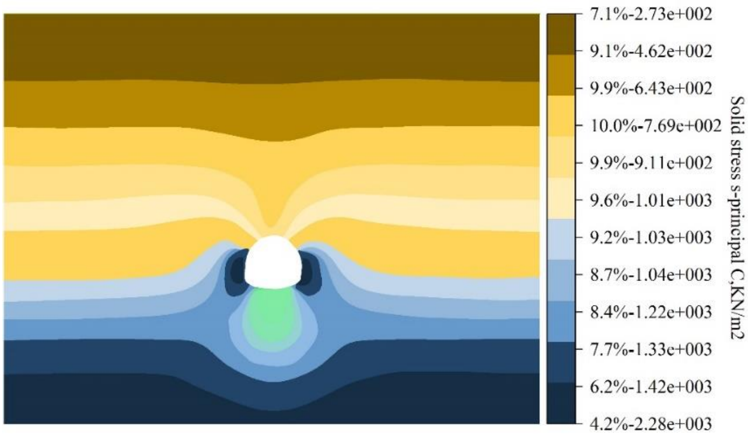

(a) Third principal stress of non-fluid solid coupling surrounding rock

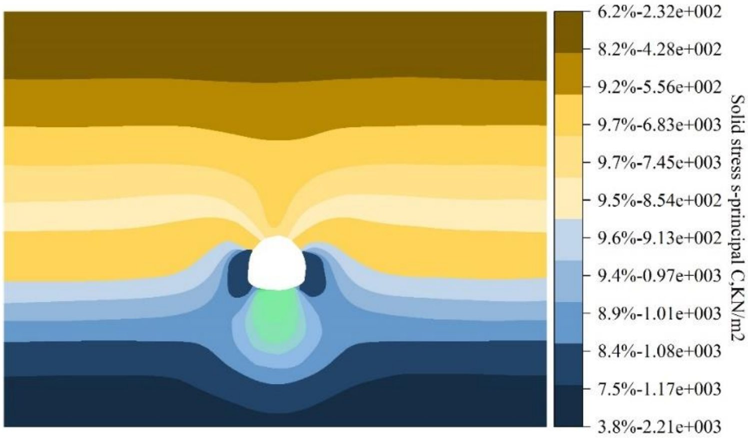

(b) Third principal stress of fluid solid coupling surrounding rock

Fig. 9. Third principal stress during tunnel excavation

Table 5 shows the distribution of the third principal stress at the critical point of the surrounding rock. From Table 5, it can be seen that whether in the fluid-solid coupling state or non-fluid-solid coupling state, the shear stress near the surrounding rock is negative, so the surrounding rock is pressurized in the excavation state. Comparing the fluid-solid coupling and non-fluid-solid coupling state, it can be seen that the fluid-solid coupling effect increases the stress of the surrounding rock, the third principal stress is 0.96MPa in the left arch waist under the non-fluid-solid coupling state, and the third principal stress is 1.43MPa under the fluid-solid coupling state, which is 1.46 times more than that of the non-fluid-solid coupling state, and the right arch waist is 1.36 times more than that of the non-fluid-solid coupling state. Compared with the non-fluid-solid coupling state, the settlement of the arch top increased by 1.50 times and the bulge of the arch bottom increased by 1.35 times in the fluid-solid coupling state. Compared with the non-fluid-solid coupling state, the left arch footing increases by 1.14 times and the right wall corner increases by 1.11 times in the fluid-solid coupling state. From the increase coefficients of each key point, it can be seen that the increase of the left and right arch footing is smaller than that of the left and right arch waist.

Table 5. Third principal stress at key points of surrounding rock (MPa)

Operating condition	Without fluid coupling	With fluid coupling	Increase factor
Vault	-0.48	-0.72	1.50
Left arch waist	-0.96	-1.43	1.46
Right arch waist	-1.01	-1.37	1.36
Left arch foot	-2.04	-2.32	1.14
Right arch foot	-1.92	-2.13	1.11
Arch bottom	-0.34	-0.46	1.35

3.4. *Factor of Safety Analysis of Perimeter Rock*

The mechanical parameters of the rock mass were reduced by gradually increasing the reduction factor and the ultimate strain method factor until the displacement around the tunnel hole showed a sudden change. In the numerical simulation, three monitoring points around the peripheral rock are recorded, which are labeled as working condition 1, working condition 2 and working condition 3. According to the calculation results, the change curves of the tunnel vault settlement, horizontal convergence, and arch bottom uplift with the discount factor are plotted, and the discount factor corresponding to the sudden change of the displacement-decrease factor change curve is the safety coefficient of the tunnel.

3.4.1. Factor of safety for perimeter rock in Case 1. Case 1 is the case without considering groundwater, and the initial ground stress field is calculated using the dry density of the rock mass. The change curve of displacement with strength reduction coefficient at the characteristic point of the tunnel for Case 1 is shown in Fig. 10. From Fig. 10, it can be seen that the trends of arch settlement and arch waist horizontal displacement are basically the same, and the deformation of the surrounding rock increases sharply when the discount factor is more than 9.03. Therefore, the tunnel safety coefficient without considering groundwater is 9.03. It should be noted that when the strength reduction factor is greater than 9.03, the tunnel arch bulge does not increase significantly, which is due to the fact that the tunnel will be damaged along the critical sliding surface in the critical state. The monitoring point of the tunnel arch bottom is below the sliding surface, which is less affected by the destabilization of the tunnel, and the growth of the arch bottom bulge is smaller.

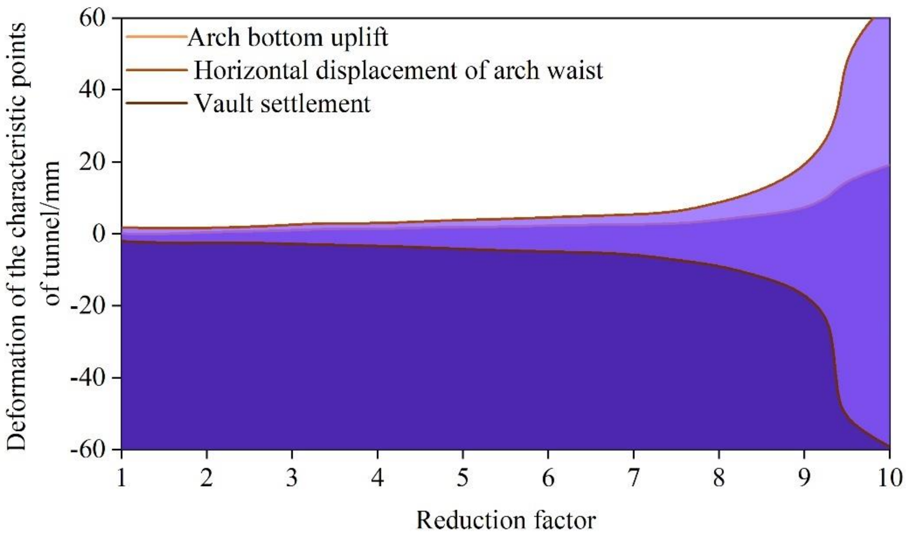

Fig. 10. Curves of displacement with reduction factor in case 1

3.4.2. Factor of safety for perimeter rock for Case 2. In Case 2, the indirect coupling mode is used to calculate the influence of groundwater seepage on the safety factor of the tunnel. The specific calculation process is as follows: firstly, turn on the seepage mode and close the mechanical process to analyze the change of seepage field caused by tunnel excavation. After the seepage field calculation is completed, the seepage mode is turned off and the fluid modulus is set to 0 (to avoid the change of pore water pressure caused by the mechanical calculation), and the mechanical process is turned on to carry out the mechanical calculation until convergence. Using this calculation mode, the pore pressure field is not coupled with the stress field, which is an approximate calculation method for calculating groundwater seepage. The variation curve of the tunnel characteristic point displacement with the discount factor under this working condition is shown in Fig. 11. Comparing Fig. 10 and Fig. 11, it can be found that the trend of tunnel deformation in Case 2 is more consistent with Case 1. The settlement of the arch and horizontal convergence are much larger than the deformation of the arch bottom bulge, and the growth of the arch bottom bulge with the strength reduction factor is not obvious. When the strength reduction factor is greater than 6.51, the settlement of the vault and the horizontal displacement of the arch girdle increase sharply, and the calculated tunnel safety factor in Case 2 is 6.51.

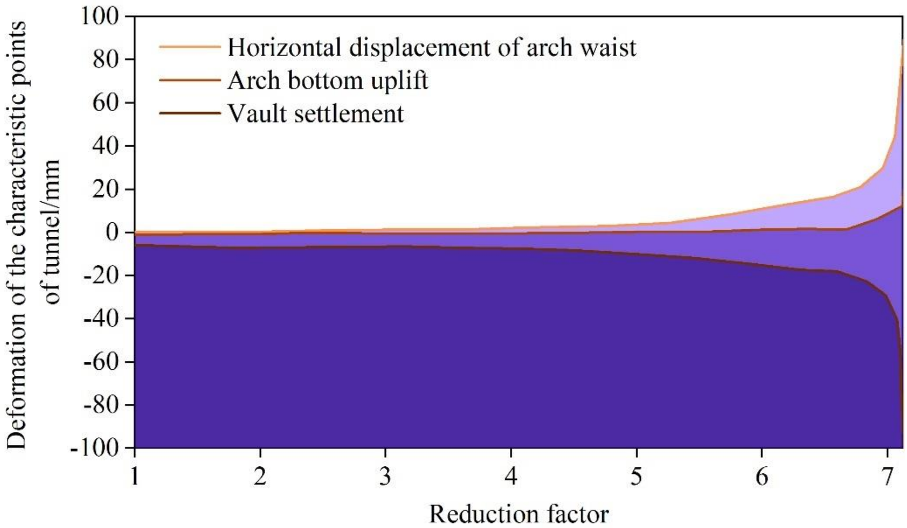

Fig. 11. Curves of displacement with reduction factor in case 2

3.4.3. Factor of safety for perimeter rock in Case 3. Case 3 utilizes the fluid-solid fully coupled model to calculate the safety factor of the tunnel when groundwater seepage occurs. When the fully coupled flow-solid model is utilized, both the fluid model and the mechanical model are in the open state, and the coupled flow-solid solution is carried out directly. In this method, each seepage time step contains a number of mechanical time steps, and each seepage time step has to reach mechanical equilibrium. In order to ensure the accuracy of the calculation, the seepage time step is small enough, so it takes a lot of calculation time. The variation curve of the tunnel characteristic point displacement with the discount factor under the working condition is shown in Fig. 12. As can be seen from Fig. 12, the settlement of the arch and the horizontal displacement of the arch girdle increase sharply when the strength reduction factor is greater than 5.18, and the safety factor of the tunnel under this condition is 5.18. Combining the safety factor and deformation of the three conditions, it can be concluded that the seepage of groundwater will significantly cause a decrease in the safety factor of the tunnel surrounding rock.

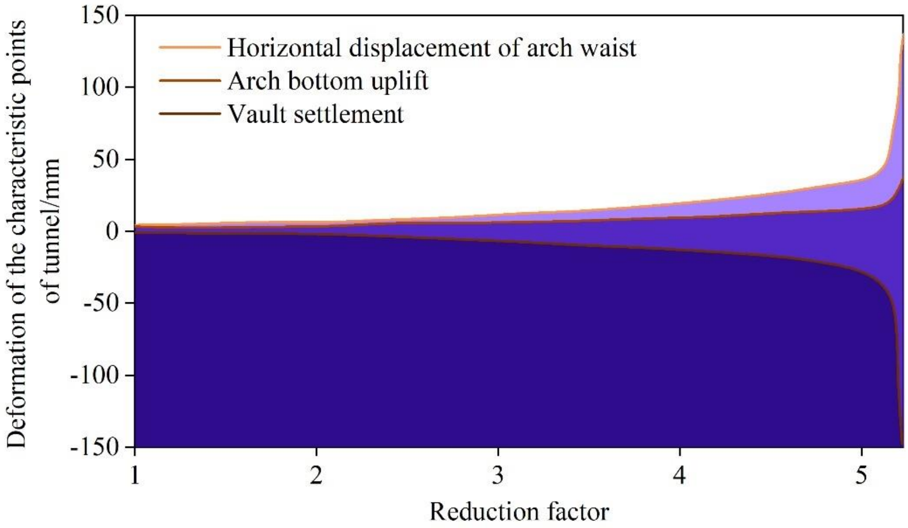

Fig. 12. Curves of displacement with reduction factor in case 3

4. Conclusion

This paper investigates the effect of groundwater seepage on the stability of foundation engineering based on the coupled flow-solid model. The tunnel is selected as the foundation project for the study to analyze the influence of groundwater seepage on the perimeter displacement of surrounding rock, strength of surrounding rock and safety index of surrounding rock in tunnel excavation.

1) The pore water pressure difference after tunnel excavation causes the seepage field around the surrounding rock to change, and under the action of groundwater seepage, the pore water pressure of the rock mass around the palm face changes from a stable horizontal distribution to a curved distribution, and eventually forms a funnel-shaped settlement zone.

2) Compared with the case without considering fluid-solid coupling, considering fluid-solid coupling increases the settlement value of the top of the arch by 1.33 times, and the augmentation of the bottom of the arch by 1.52 times. Horizontally, the horizontal displacement of the left wall increases by 1.14 times and that of the right wall increases by 1.33 times due to fluid-solid coupling. And the analysis shows that the fluid-solid coupling effect generated by groundwater seepage makes the vertical displacement increase coefficient of tunnel excavation larger than the horizontal displacement increase coefficient.

3) The peripheral rock stress is similar to that without considering the fluid-solid coupling effect, but there is a change in the numerical value. The peripheral rock stress at the left arch waist increases by 1.46 times in the fluid-solid coupling condition compared with the non-fluid-solid coupling condition, and increases by 1.36 times at the right arch waist, and the rest of the key positions have different degrees of increase.

4) When groundwater is not considered, the perimeter rock safety coefficient reaches 9.03, but after considering the seepage of groundwater, the perimeter rock safety coefficient finally decreases to 5.18, which indicates that the seepage of groundwater will significantly cause the decrease of the perimeter rock safety coefficient of the tunnel, which is a serious threat to the stability of the tunnel.

Funding

This work was supported by Natural Science Foundation of Henan Province, China (242300420316).

References

[1] Ouzaid, I., Benmebarek, N., & Benmebarek, S. (2020). FEM optimisation of seepage control system used for base stability of excavation. Civil Engineering Journal, 6(9), 1739-1751.

[2] Ramkrishnan, R., Karthik, V., Unnithan, M. S., Balaji, R. K., Vinu, M. A., & Venugopalan, A. (2017). Stabilization of seepage induced soil mass movements using sand drains. Geotech. Eng. J. SEAGS & AGSSEA, 48(4), 129-137.

[3] Jin, L., Wei, J., Luo, C., & Qin, T. (2023). Slope stability analysis based on improved radial movement optimization considering seepage effect. Alexandria Engineering Journal, 79, 591-607.

[4] Li, Y., Chai, J., & Xu, Z. (2017, June). Analysis of influence of seepage on stability of foundation pit. In IOP Conference Series: Materials Science and Engineering (Vol. 207, No. 1, p. 012093). IOP Publishing.

[5] Cheng, X., Zhang, X., Chen, W., Xu, W., & Du, X. (2017). Stability analysis of a cross-sea tunnel structure under seepage and a bidirectional earthquake. International Journal of Geomechanics, 17(9), 06017008.

[6] Liu, J., Yang, C., Gan, J., Liu, Y., Wei, L., & Xie, Q. (2017). Stability analysis of road embankment slope subjected to rainfall considering runoff-unsaturated seepage and unsaturated fluid–solid coupling. International Journal of Civil Engineering, 15, 865-876.

[7] He, Z. M., Tang, H. L., & Deng, X. (2018). Effect of Seepage Force on Stability of High Embankment with Coarse-Grained Soil during Rainfall. Journal of Highway and Transportation Research and Development (English Edition), 12(1), 44-52.

[8] Salahudeen, A. B., & Yisa, G. L. (2023). Settlement, slope stability and seepage analyses By Numerical Modelling Method and their applications in practice. Nigerian Journal of Technology, 42(3), 306-314.

[9] Zou, J. F., & Qian, Z. H. (2018). Face-stability analysis of tunnels excavated below groundwater considering coupled flow deformation. International Journal of Geomechanics, 18(8), 04018089.

[10] Belew, A. Z., Tenagashaw, D. Y., Ayele, W. T., & Andualem, T. G. (2022). Coupled analysis of seepage and slope stability: a case study of ribb embankment dam, Ethiopia. Water Conservation Science and Engineering, 7(3), 293-314.

[11] Bhattacharya, P., & Dutta, P. (2023). Stability of rectangular tunnel in anisotropic cohesionless soil under steady-state groundwater flow. European Journal of Environmental and Civil Engineering, 27(4), 1596-1616.

[12] Li, S., Wu, N., & Liu, G. (2022). Stability analysis of slopes subjected to transient unsaturated seepage effect considering hydromechanical coupling effect. International Journal of Geomechanics, 22(6), 04022078.

[13] Liu, C., Shen, Z., Gan, L., Xu, L., Zhang, K., & Jin, T. (2018). The seepage and stability performance assessment of a new drainage system to increase the height of a tailings dam. Applied Sciences, 8(10), 1840.

[14] Zhang, L., Ying, H., Wang, D., Xie, K., & Zhu, C. W. (2018, August). Seepage Stability Calculation of Excavation Base due to Groundwater Level Fluctuation. In Proceedings of China-Europe Conference on Geotechnical Engineering: Volume 2 (pp. 1098-1101). Cham: Springer International Publishing.

[15] Ismail, M. A. M., Ng, S. M., & Abustan, I. (2017). Parametric study of horizontal drains for slope stability measure: A case study in Putrajaya, Malaysia. KSCE Journal of Civil Engineering, 21, 2162-2167.

[16] Deng, D. P., Li, L., & Zhao, L. H. (2019). Stability analysis of slopes under groundwater seepage and application of charts for optimization of drainage design. Geomech. Eng, 17(2), 181-194.

[17] Zhou, C. B., Chen, Y. F., Hu, R., & Yang, Z. (2023). Groundwater flow through fractured rocks and seepage control in geotechnical engineering: Theories and practices. Journal of Rock Mechanics and Geotechnical Engineering, 15(1), 1-36.

[18] Wei, Z., & Zhu, Y. (2021). A theoretical calculation method of ground settlement based on a groundwater seepage and drainage model in tunnel engineering. Sustainability, 13(5), 2733.

[19] Di, Q., Li, P., Zhang, M., Zhang, W., & Wang, X. (2022). Analysis of face stability for tunnels under seepage flow in the saturated ground. Ocean Engineering, 266, 112674.

[20] Li, L., Tu, W., Zhou, Z., Shi, S., Zhang, M., & Chen, Y. (2020). Dynamic unloading instability mechanism of underground cavern based on seepage-damage coupling. KSCE Journal of Civil Engineering, 24, 1620-1631.

[21] MI, B., & XIANG, Y. Y. (2020). Model experiment and calculation analysis of excavation-seepage stability for shallow shield tunneling in sandy ground. Rock and Soil Mechanics, 41(3), 4.

[22] J. Apraiz,A. Doubova,E. Fernández Cara & M. Yamamoto. (2024). Inverse Problems for One-Dimensional Fluid-Solid Interaction Models. Communications on Applied Mathematics and Computation(prepublish),1-15.

[23] Theinat Audai,Salgado Rodrigo,Prezzi Monica & Sakleshpur Venkata A. (2024). Stability and Factor of Safety of Gravity-Retaining Structures Using the Strength Reduction Method. Journal of Geotechnical and Geoenvironmental Engineering(12),

[24] Ren Yiwei,Zhou Shijun,Jia Jiayin,Yuan Qiang,Zhou Zelin,Liu Maoyi & He Huayong. (2023). Construction stability analysis of intersection tunnel in city under CRD method. Frontiers in Earth Science.

[25] Jianping Xin,Yingren Zheng,Yingxiang Wu & Abi Erdi. (2017). Analysis of Tensile Strength's Influence on Limit Height and Active Earth Pressure of Slope Based on Ultimate Strain Method. Advances in Materials Science and Engineering1-8.